Exploitation of Induction Machine's High-Frequency Behavior for Online Insulation Monitoring

Peter Nussbaumer, Markus A. Vogelsberger, Thomas M. Wolbank

Abstract -- **The trend to increased energy efficiency and profitable capital expenditure leads to the operation of drive systems at or near their rated values and to increased running time. Thus, down time due to machine breakdown (e.g. in a traction drive) leads to high economic losses for the operator. Furthermore, the breakdown of safety-critical devices may lead to dangerous situations. Due to the above stated reasons the demand for operation reliability is constantly increasing.**

The fast switching of the voltage source inverter (VSI) in adjustable speed drives (ASD) leads to increased stress for the winding insulation. Thus, it gets even more important to monitor the condition of the insulation in inverter-fed drives.

Degradation of the insulation results in an alteration of the machine's high-frequency behavior. The proposed method is capable of detecting such changes by evaluation of the transient current reaction on inverter switching.

Index Terms--**AC motor drives, Fault diagnosis, Induction motor protection, Monitoring, Pulse width modulated inverters, Rotating machine insulation testing, Squirrel cage motors**

I. Introduction

IN modern traction drives the application of adjustable speed drives consisting of an AC machine (typically induction or permanent magnet synchronous (PMSM) machine) and inverters (nowadays voltage source inverters with IGBTs (Insulated Gate Bipolar Transistors)) is standard. Although electrical machines are generally highly reliable the increased demand of system availability leads to the necessity to implement condition monitoring, fault detection and/or fault tolerant control.

The main causes for machine breakdown have been analyzed in [1] and [2]. The result is that machine breakdown originates in faults that can be classified in three categories – bearing, stator and rotor related faults. According to these investigations the second most common causes are stator related accounting for about 35% of all collected machine breakdowns. Within these stator related faults problems with the insulation leading to short circuit faults account for 70%. Thus, reliable monitoring of the insulation condition allows the shift of maintenance strategy from preventive to predictive. In case of predictive maintenance, the risk of failure estimated by insulation condition monitoring allows to decide if maintenance (e.g. replacement of the windings before breakdown of the insulation system) is required or not.

Usually breakdown of the insulation is a slowly developing process starting with deterioration of the insulation material and then leading to severe turn-to-turn, phase-to-phase or phase-to-ground short circuits [3]. The exact time of insulation breakdown cannot be determined according to [4]. Therefore only a risk of failure rather than a time to failure can be defined.

The deterioration of the insulation condition is accelerated by different causes. The main cause according to [5] is thermal stress. However, electrical, mechanical and environmental strains lead to deterioration of the insulation material too. Concerning inverter-fed drives the fast rise times of modern switching devices like IGBTs and MOSFETs leads to increased electrical stress of the insulation system as analyzed in [3].

So far, many different insulation fault detection and condition monitoring techniques have been proposed in literature. All methods can be categorized into offline or online approaches. The most industrially accepted methods are applied offline. Thus the machine has to be taken out of service to test its insulation.

The offline partial discharge [8] and offline surge [6] test are able to detect insulation deterioration. Further offline insulation fault detection techniques are the DC conductivity test [7], the insulation resistance (IR) test [4], DC/AC HiPot test [4] and polarization index (PI) test [4].

So far the only industrially accepted online insulation monitoring technique is the online partial discharge (PD) test [9]. However, this test is only applicable for medium to high voltage machines and needs additional measurement hardware and highly sophisticated evaluation software. Many other online insulation fault detection methods have been presented in literature. However, most of them are only able to detect solid stator faults but no insulation deterioration. The approach to use motor current signature analysis (MCSA) for insulation fault detection is presented for example in [10]. The adaption of the surge test for online applicability is proposed in [11]. This test is design for application in mains-fed machines. Evaluation of the transient leakage induction by measuring the current reaction on inverter switching is presented in [12] to detect solid turn-to-turn faults.

The requirements of the presented online insulation monitoring method are applicability for inverter-fed drives, usage of the already available sensors only, the detection of

The work to this investigation was supported by the Austrian Science Fund (FWF) under grant number P23496-N24.

P. Nussbaumer and T.M. Wolbank are with the Institute of Energy Systems and Electrical Drives, Vienna University of Technology, 1040 Vienna, Austria (e-mail: peter.nussbaumer@tuwien.ac.at; thomas.wolbank@tuwien.ac.at)

M.A. Vogelsberger is with Bombardier Transportation Austria GmbH, Drives Development Center, PPC, 1220 Vienna, Austria (e-mail: markus.vogelsberger@at.transport.bombardier.com)

978-1-4799-0025-1/13/$31.00 ©2013 IEEE

insulation deterioration and that no disassembling of the drive is necessary.

This paper briefly presents the developed online insulation monitoring method and compares its application to two different induction machine drive systems with different power ratings in experimental investigations. Furthermore the application of the method for different DC-link voltage values but same machine is compared.

II. High-Frequency Behavior of Inverter-Fed Drives

The fast voltage rise times of modern switching devices additionally stresses the winding insulation as mentioned in the introduction. The cause for this stress is the occuring transient overvoltage resulting from reflections of the applied voltage pulse at the machine's terminal connections. According to traveling wave theory the mismatch of machine and supply cable impedance leads to these reflections [13]. The machine impedance is by far bigger than the cable impedance. Thus, in theory the voltage pulse is fully reflected (reflection coefficient nearly one) [13]. The reflected voltage pulse leads to an oscillating transient overvoltage with decaying magnitude. The peak value can reach up to twice or even four times (for fast subsequent voltage pulses) the DC-link voltage and the oscillation frequency is in the range of tens kHz to tens MHz [14].

An inverter-fed drive system consists of three main components defining the complex impedance system leading to the voltage pulse reflections:

- Inverter (e.g. voltage source inverter)
- Supply cables
- AC machine (e.g. induction machine)

The elements defining the characteristic of the drive's behavior like stator resistance r_S, stator inductance l_S, cable inductance and resistance per unit length, etc. on the one hand and the parasitic components like phase-to-ground (cable), winding-to-ground (machine), winding-to-winding (machine) and turn-to-turn (machine) capacitance and the inverter's capacitive coupling to ground on the other hand determine the mentioned drive's complex impedance network. Many of the parasitic components are defined and strongly influenced by the insulation system. Thus, these components also influence the oscillating transient voltage. This oscillation is also visible in the current immediately after inverter switching. It is characteristic for the machine's high-frequency behavior.

A change in the machine's insulation system (e.g. due to deterioration) leads to a change in this characteristic oscillation (hf-behavior). The proposed condition monitoring method evaluates the oscillation in the current reaction on voltage switching to detect changes in the machine's hf-behavior. It is preferred to analyze the changes in the current oscillation as current sensors are already available in modern drive systems for machine control.

III. Measurement Procedure and Signal Processing

For the evaluation of the hf-oscillation the current has to be acquired with sufficient resolution in time. The excitation of the machine in the hf-range is carried out by application of different changes of the inverter's switching state.

The used transitions of switching states always originate in the lower short circuit (-SC, 000) and end in one of the three positive active switching states (+U, 001; +V, 010; +W, 100). Standard industrial current sensor can be used (bandwidth in the range of 100kHz to 300kHz).

The current's reaction during the switching transition in phase U (-SC to +U) is depicted in Fig. 1.

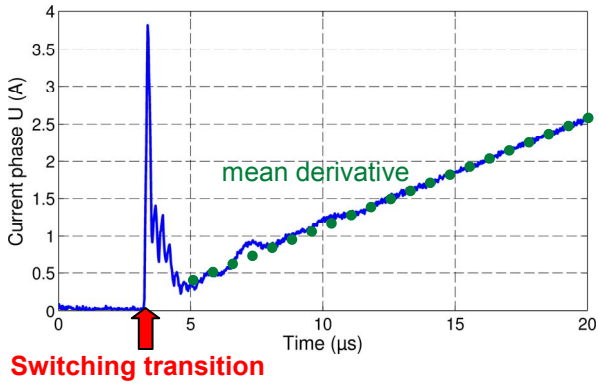

Fig. 1. Current signal with illustrated mean derivative (green, dotted line) and switching instant (red arrow).

The visible current derivative after the switching transition (denoted as mean derivative) is mainly determined by the machine's transient leakage inductance. This transient leakage inductance depends on inherent machine saliencies like rotor slotting and saturation level. Thus, this influence has to be eliminated as only the high-frequency oscillation is of interest. The elimination can be done by simply subtracting the mean derivative after exact detection of the real switching instant. The resulting signal is shown in Fig. 2

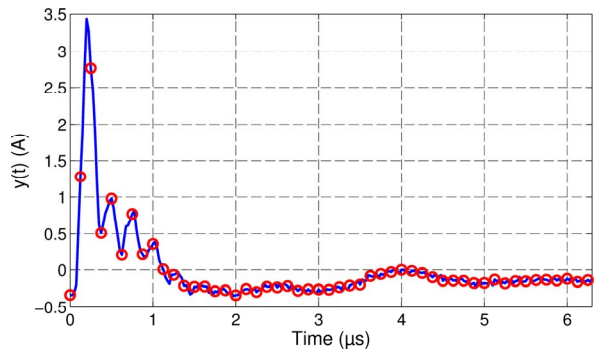

Fig. 2. Current (mean derivative subtracted) after switching transition from lower short circuit (-SC, 000) to +U (001).

The red circles highlight exemplary sampling instants. The transient current oscillation depicted above is further analyzed in the frequency domain. Therefore the depicted signal is transformed by FFT (Fast Fourier Transform). The investigated time window is chosen from the real switching

instant until the oscillation has decayed. For the shown signal this time window is chosen to 6.4µs. The used sampling frequency is 40MS/s. Thus the number of sample values equals to *N=256*. The resulting amplitude spectrum after Fourier transform is depicted in Fig. 3 for evaluation in phase U.

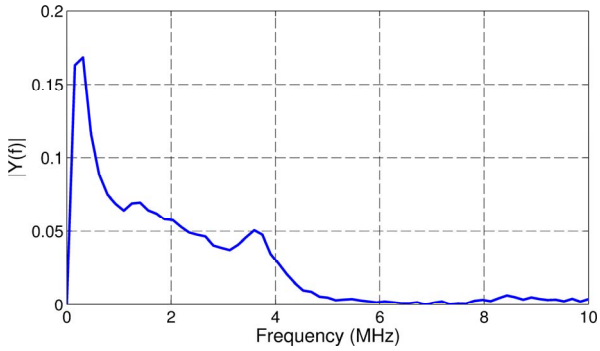

Fig. 3. Amplitude spectrum of measured current in phase U after switching transition from lower short circuit (-SC, 000) to +U (001).

The amplitude spectrum is characteristic for the machine's hf-behavior in phase U. If recorded for healthy machine condition it serves as a reference trace and is compared to later measurements to assess the machine's insulation condition in the proposed monitoring method. To detect changes in the machine's hf-behavior the above described measurement procedure and signal processing is repeated for all three phases. For each of the three phases a reference amplitude spectrum (recorded for healthy machine condition) is stored for later comparison to condition measurements and assessment of the insulation condition.

IV. Insulation State Indicator (ISI/SISI)

The measurement and signal processing has been described in the previous section. An insulation state indicator is introduced for the assessment of the insulation condition in one phase. It is based on quantifying the change in the machine's high-frequency behavior by comparison of amplitude spectrum recorded for healthy machine condition (reference) and during condition assessment. The Root Mean Square Deviation (RMSD) is chosen as a comparative value and serves as Insulation State Indicator (ISI) for the respective phase.

$$ISI_{p,k} = RMSD_{p,k}(x_1, x_2) = \frac{\sqrt{\sum_{i=n_{low}}^{n_{high}} \left(Y_{ref,p}(i) - \left|Y_{con,p,k}(i)\right|\right)^2}}{n_{high} - n_{low}} \quad (1)$$

The Fourier transformed signals Y_{ref} and Y_{con} have been obtained by the procedure described in section III. for healthy machine condition and a later condition measurement, respectively. The index p defines the investigated phase (U,V,W). The variables n_{high} and n_{low} define the compared frequency range and depend on sampling rate and investigated window length. The definition of the evaluated frequency range allows separating other influences like cabling or grounding leading to a change in the drive's high-frequency behavior. Due to the fact that a single measurement's duration is in the range of a few hundred microseconds the procedure can be repeated *m*-times to increase the accuracy of the method. Thus, the index k (1,2,3,…) denotes the number of the consecutive measurements.

The used reference signal (frequency spectrum for healthy machine condition) is the mean trace calculated from *m* measurements.

$$Y_{ref}(i) = \frac{\sum_{k=1}^{m} \left|Y_{ref,k}(i)\right|}{m} \quad (2)$$

The variable i identifies the discrete frequency. The frequency is calculated using the sampling rate f_S, the number of samples N and the window length t_{win} according to the following equation

$$f = \frac{i \cdot f_s}{N};\ i = 0,1,2,3,...;\ N = t_{win} \cdot f_s \quad (3)$$

The quantity defining the insulation condition in one phase is the insulation state indicator ISI_p calculated from *m* RMSD values according to equation (1).

$$ISI_p = \frac{\sum_{k=1}^{m} ISI_{p,k}}{m} \quad (4)$$

In a last step of signal processing a Spatial Insulation State Indicator (SISI) is calculated by linear combination of the ISI values of all three phases.

$$SISI = ISI_U + ISI_V \cdot e^{j\frac{2\pi}{3}} + ISI_W \cdot e^{j\frac{4\pi}{3}} \quad (5)$$

Symmetrical changes of the high-frequency behavior (e.g. due to temperature variation, change of cabling,…) are eliminated by this linear combination as these lead to a zero-sequence component. The successful elimination of influences on the insulation state indicator due to the cable has been given in [15] by the authors.

V. Experimental Setup

The main focus in this paper is to compare the applicability of the above proposed condition monitoring method on induction machines with clear different power rating and insulation systems. Thus two different machines have been investigated. Induction machine IM#1 is a industrial 2-pole machine with 5.5kW and enamel-insulated wire. Induction machine IM#2 on the other hand is a 4-pole 1.4MW machine with fibre-insulation wires. Both machines have a squirrel cage rotor and several tapped windings accessible at the machine's terminal connection block. Thus, it is possible to change the machine's hf-behavior by inserting capacitors between the different taps of the winding. The exemplary scheme of the parasitic capacitances (turn-to-turn $C_{t\text{-}t}$, phase-to-phase $C_{ph\text{-}ph}$, phase-to-ground $C_{ph\text{-}gnd}$) in the machine and this additional capacitor C_{fault} are depicted in Fig. 4. The phase-to-ground capacitances of IM#1 and IM#2 are 1.5nF and 21nF respectively. The additional capacitor in parallel to the turn-

to-turn capacitances results in an increase. This is in accordance to the results of increasing capacitance due to insulation deterioration presented in [16].

The measurements, control and signal processing are carried out with a combined system of Real-Time processor, Field Programmable Gate Array (FPGA) and fast sampling ADCs from National Instruments, programmable in LabVIEW.

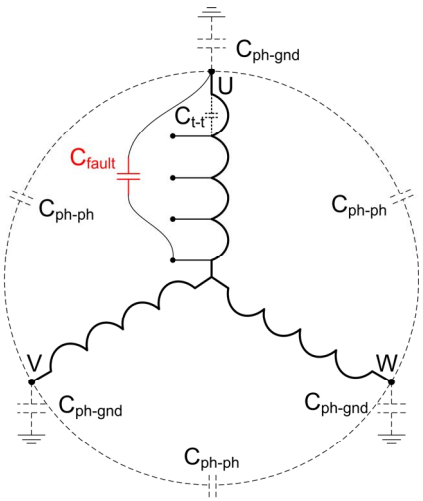

Fig. 4. Additional capacitor C_{fault} inserted in parallel to the full phase winding U, schemetically.

VI. Experimental Results

The purpose of the following experimental investigations is to identify differences in the application of the above presented monitoring method between induction machines with different power rating and insulation system.

In a first step the differences in the high-frequency behavior of the two investigated machines is analyzed regarding the amplitude spectrum for health insulation condition. Fig. 5 shows this comparison of the amplitude spectrum normalized on the respective maximum magnitude of each machine.

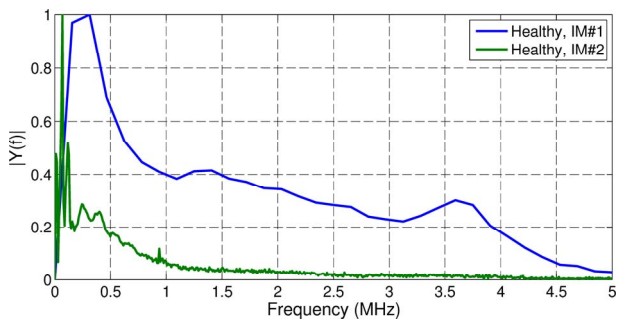

Fig. 5. Normalized Amplitude spectrum of measured current in phase U after switching transition from lower short circuit (000) to +U (001) for induction machine IM#1 (blue) and IM#2 (green).

It is clearly visible that the dominant frequencies for the machine with higher power rating (IM#2) are in a lower frequency range than the ones of IM#1. The highest magnitude can be identified at 313kHz and 68kHz for induction machine IM#1 and IM#2, respectively.

The sampling rate in both investigations is chosen 40MS/s. The investigated time window length t_{win} is defined to 6.4µs and 102.4µs for IM#1 and IM#2, respectively. The time window depends on the duration of the decaying transient oscillation visible in the current signal. The DC link voltage (voltage pulse magnitude) in case of IM#1 is 440V, in case of IM#2 it is 600V.

In a next investigation an additional capacitor is inserted in parallel to the full phase winding U. The value of the inserted capacitor is chosen with respect to the phase-to-ground capacitance of the two machines IM#1 and IM#2 to 0.5nF and 15nF, respectively. The amplitude spectra for the reference signal in phase U, $Y_{ref,U}$ (according to (2)) is compared to the amplitude during a condition measurement $|Y_{con,U,1}|$. This comparison and the resulting square deviation is depicted in Fig. 6 and Fig. 7 for induction machine IM#1 and IM#2, respectively.

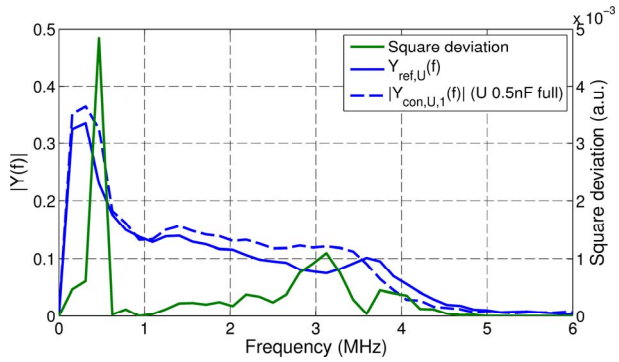

Fig. 6. Reference amplitude spectrum $Y_{ref,U}(f)$ (blue, solid trace), amplitude spectrum of one condition assessment $|Y_{con,U,1}(f)|$ (blue, dashed trace) for 0.5nF capacitor inserted in parallel to the full winding of phase U and calculated square deviation of both traces (green, solid trace); IM#1.

For both investigated machines a dominant change in specific frequency components can be detected.

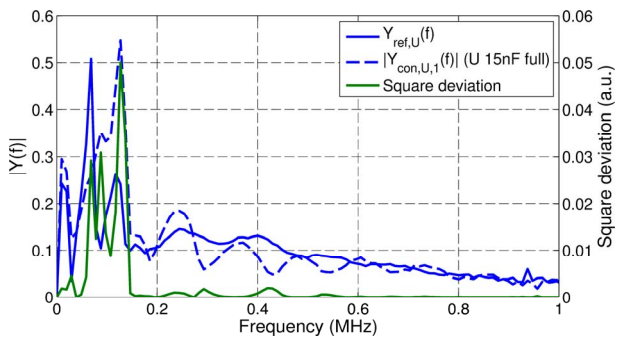

Fig. 7. Reference amplitude spectrum $Y_{ref,U}(f)$ (blue, solid trace), amplitude spectrum of one condition assessment $|Y_{con,U,1}(f)|$ (blue, dashed trace) for 15nF capacitor inserted in parallel to the full winding of phase U and calculated square deviation of both traces (green, solid trace); IM#2, U_{DC}=600V.

For IM#1 this change is at 469kHz. Whereas the most dominant changes for IM#2 can be detected at 68kHz,

88kHz and 127kHz.

Concerning induction machine IM#2 the influence of DC-link voltage on the dominant frequencies and the interesting frequencies in case of changed hf-behavior were investigated next. The results for investigations with DC-link voltage of 600V are already shown in Fig. 7. The results for the same evaluation but a DC-link voltage of 2800V are illustrated in Fig. 8.

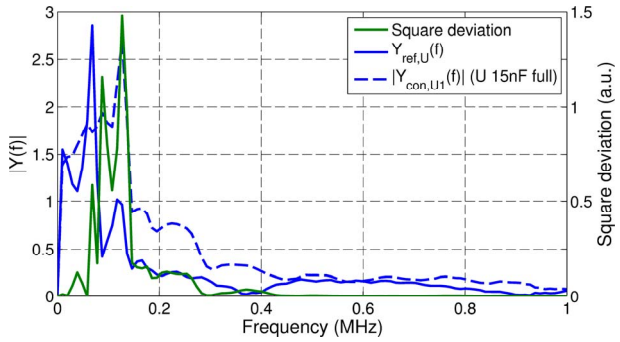

Fig. 8. Reference amplitude spectrum $Y_{ref,U}(f)$ (blue, solid trace), amplitude spectrum of one condition assessment $|Y_{con,U,1}(f)|$ (blue, dashed trace) for 15nF capacitor inserted in parallel to the full winding of phase U and calculated square deviation of both traces (green, solid trace); IM#2, U_{DC}=2800V.

The most dominant frequency component in case of healthy machine condition is identified to 68kHz and the interesting frequency components for changed hf-behavior of the machine are 68kHz, 88kHz and 127kHz. Thus, all regarded frequency component are the same for both scenarios. Therefore the magnitude of the DC-link voltage does not significantly influence the frequency of the transient current oscillation.

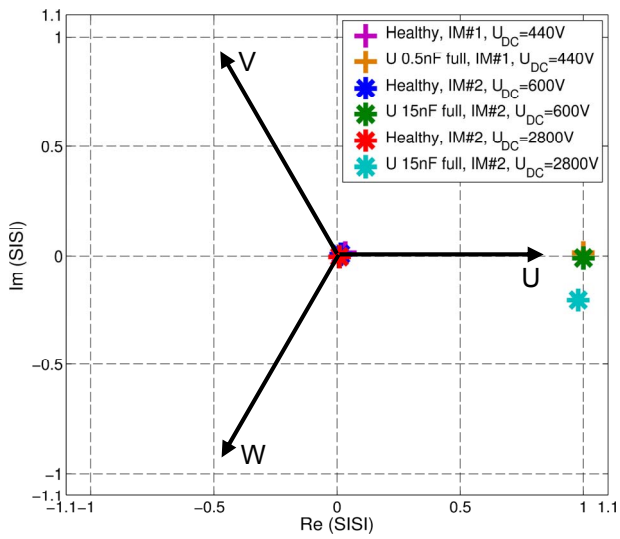

Fig. 9. Normalized spatial insulation state indicator (SISI) for different investigated machines (IM#1 and IM#2) and changed hf-behavior.

At the end of insulation condition assessment using the proposed monitoring method the spatial insulation state indicator calculated according to equation (5) is regarded. This indicator is depicted in Fig. 9 for the above investigated scenarios. For all scenarios the indicator is normalized on the magnitude of the respective SISI for changed machine's hf-properties. It is shown that in all investigated scenarios the changed machine condition is clearly different to the unchanged ('Healthy') one. The unchanged machine condition always results in a spatial insulations state indictor in or close to the origin of the Gaussian plane. The capacitor has been inserted in phase U for all scenarios. The SISI is pointing in direction of phase axis U. Thus, the phase location of the alteration can be identified. In case of investigated induction machine IM#2 and DC-link voltage of 2800V the angle of the spatial insulation state indicator is approximately 10°. This deviation from the other scenarios (angle equaling ~0°) will be further investigated in future measurements.

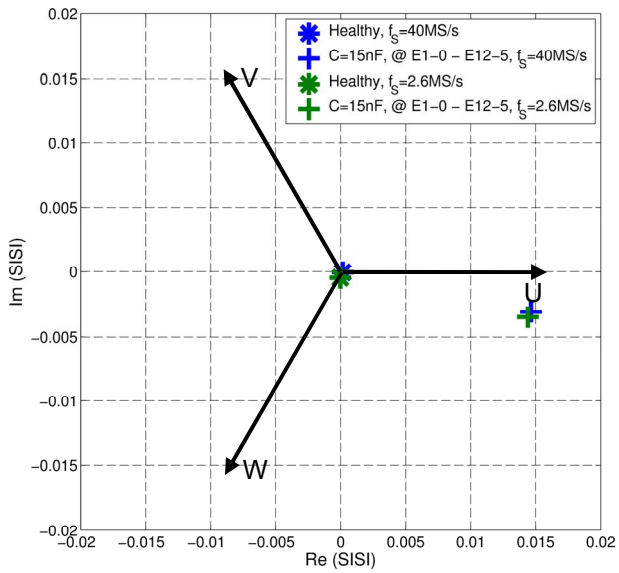

Fig. 10. Spatial insulation state indicator (SISI) for induction machine IM#2 (UDC=2800V); sampling rate f_S equals 40MS/s (blue) and 2.6MS/s (green).

An important parameter concerning the implementation of the proposed condition monitoring technique is the sampling rate needed for accurate calculation of the insulation state indicator. The above presented investigations have been carried out with a sampling rate of 40MS/s. In modern drive systems the sampling rate of the used analog-to-digital converters (ADCs) is lower. Thus, investigations concerning the necessary sampling rate have been carried out on induction machine IM#1. The results have been presented in [17]. The conclusion has been that the necessary sampling rate depends on the frequency range investigated for calculation of the insulation state indicator. The sampling rate has to be 20-times higher than the highest interesting frequency. This results in a necessary sampling rate of 10MS/s in case of induction machine IM#1 as the interesting frequency is about 500kHz. In case of induction machine

IM#2 the highest interesting frequency is lower and can be identified to about 130kHz. According to the above mentioned rule of thumb the necessary sampling rate results to 2.6MS/s. The obtained spatial insulation state indicators for induction machine IM#2 and DC-link voltage of 2800V at different sampling rates (40MS/s and 2.6MS/s) are depicted in Fig. 10. It can be seen that the resulting indicators are almost identical for both investigated scenarios and sampling rates. Thus a reduction of the sampling rate to 10MS/s (IM#1) and 2.6MS/s (IM#2) can be made according to the rule of thumb presented in [17] without deterioration in accuracy.

VII. Conclusions

Insulation deterioration influences the machine's high-frequency behavior. Thus, a condition monitoring method has been developed and presented that is capable of detecting such changes by evaluation of the transient current reaction immediately after inverters switching. The method has been applied to a small 5.5kW and a bigger 1.4MW induction machine both with different insulation systems. The results have been compared for different machine ratings and different DC-link voltages. It is concluded that the method can be applied to machines with different power ratings as well as insulation systems. Furthermore DC-link voltage does not influence the frequency range investigated during the calculation of the insulation state indicator.

Sampling rate used for current acquisition is a crucial parameter in the design of the measurement hardware needed for the condition monitoring method. Thus, an analysis of the necessary sampling rate has been carried out and compared to previous results. The sampling rate has to be approximately 20-times higher than the maximum frequency component used for the calculation of the insulation state indicator.

VIII. Acknowledgment

The authors want to thank Bombardier Transportion Switzerland, Converter Department (head Markus Jörg, MSc) and especially the team of BT-Powerlab Zürich for the generous support. Special thanks also goes to National Instruments Austria and especially DI Günther Stefan for the generous support and donation to finance the measurement hardware.

IX. References

[1] IEEE Committee Report; "Report of large motor reliability survey of industrial and commercial installation, Part I," *IEEE Trans. on Ind. Appl.,* vol.21, no.4, pp.853–864, 1985.

[2] IEEE Committee Report; "Report of large motor reliability survey of industrial and commercial installation, Part II," *IEEE Trans. on Ind. Appl.,* vol.21, no.4, pp.865–872, 1985.

[3] Yang, J; Cho, J.; Lee, S.B.; Yoo, J.-Y.; Kim, H.D.; "An Advanced Stator Winding Insulation Quality Assessment Technique for Inverter-Fed Machines," *IEEE Trans. on Ind. Appl.,* vol.44, no.2, pp.555-564, 2008.

[4] Stone, G.C.; Boulter, E.A.; Culbert, I.; Dhirani, H.; "Electrical Insulation for Rotating Machines," IEEE Press, Wiley & Sons, 2004.

[5] Grubic, S.; Aller, J.M.; Bin Lu; Habetler, T.G.; "A Survey on Testing and Monitoring Methods for Stator Insulation Systems of Low-Voltage Induction Machines Focusing on Turn Insulation Problems," *IEEE Trans. on Industrial Electronics,* vol.55, no.12, pp.4127-4136, 2008.

[6] Wiedenbrug, E.; Frey, G.; Wilson, J.; "Impulse testing and turn insulation deterioration in electric motors," *Annual Pulp and Paper Industry Technical Conference,* pp. 50- 55, 2003.

[7] Schump, D.E.; "Testing to assure reliable operation of electric motors," *Industry Applications Society 37th Annual Petroleum and Chemical Industry Conference,* pp.179-184, 1990.

[8] Stone, G.C.; "Recent important changes in IEEE motor and generator winding insulation diagnostic testing standards," *IEEE Trans. on Ind. Appl.,* vol.41, no.1, pp. 91-100, 2005.

[9] Stone, G.C.; Sedding, H.G.; Costello, M.J.; "Application of partial discharge testing to motor and generator stator winding maintenance," *IEEE Trans. on Ind. Appl.,* vol.32, no.2, pp.459-464, 1996.

[10] Nandi, S.; Toliyat, H.A.; "Novel frequency-domain-based technique to detect stator interturn faults in induction machines using stator-induced voltages after switch-off," *IEEE Trans. on Ind. Appl.,* vol.38, no.1, pp.101-109, 2002.

[11] Grubic, S.; Habetler, T.G.; Restrepo, J.; "A new concept for online surge testing for the detection of winding insulation deterioration," *Energy Conversion Congress and Exposition (ECCE),* pp.2747-2754, 2010.

[12] Wolbank, T.M.; Wohrnschimmel, R.; "Transient electrical current response evaluation in order to detect stator winding interturn faults of inverter fed ac drives," *Symposium on Diagnostics for Electric Machines, Power Electronics and Drives (SDEMPED),* pp.1-6, 2001.

[13] Kerkman, R.J.; Leggate, D.; Skibinski, G.L.; "Interaction of drive modulation and cable parameters on AC motor transients," *IEEE Trans. on Ind.Appl.,* vol. 33, pp. 722-731, 1997.

[14] Peroutka, Z. and Kus, V.; "Adverse effects in voltage source inverter-fed drive systems," *Seventeenth Annual IEEE Applied Power Electronics Conference and Exposition, APEC,* pp. 557-563, 2002.

[15] Nussbaumer, P.; Wolbank, T.M.; Vogelsberger, M.A.; "Separation of disturbing influences on induction machine's high-frequency behavior to ensure accurate insulation condition monitoring," *Twenty-Eighth Annual IEEE Applied Power Electronics Conference and Exposition (APEC),* pp.1158-1163, 2013.

[16] Perisse, F.; Werynski, P.; Roger, D.; "A New Method for AC Machine Turn Insulation Diagnostic Based on High Frequency Resonances," *IEEE Trans. on Diel. and El. Ins.,* vol.14, no.5, pp.1308-1315, 2007.

[17] Nussbaumer, P.; Vogelsberger, M.A.; Wolbank, Th.M.; "Sensitivity Analysis of Insulation State Indicator in Dependence of Sampling Rate and Bit Resolution to Define Hardware Requirements," *International Conference on Industrial Technology (ICIT),* pp.392-397, 2013.

X. Biographies

Peter Nussbaumer (SM' 2011) received the MSc degree in Power Engineering and the PhD. degree in Electrical Engineering from Vienna University of Technology, Vienna, Austria in 2009 and 2013, respectively. He is currently a Project Assistant at the Institute of Energy Systems and Electrical Drives, Vienna University of Technology and a colleague in the doctoral program Energy Systems 2030. He is engaged in several industrial and scientific projects with focus on electrical drives and electric mobility. His special fields of interest are fault detection, condition monitoring and sensorless control of inverter-fed AC machines.

Markus A. Vogelsberger received the the Dipl.-Ing./M.S. (with honor) and Dr.Techn/Ph.D. (with honor) degrees in Electrical Engineering from Vienna University of Technology, Vienna, Austria, in 2004 and 2009, respectively. He has been a Scientific Research Assistant in the Institute of Electrical Drives and Machines, Vienna University of Technology, where he has been engaged in several industrial and scientific R&D projects in the field of sensorless control, drives systems and power electronics / drive converter.
In 2011, he joined Bombardier Transportation, Vienna, Austria, as a Research & Development Engineer in the PPC-Drives Department.
His field of interest include design of traction motors, power electronics as well as control and simulation of electrical drives.
In particular, currently his focus as R&D-Project Lead for drives is on the research and development of fault detection and condition monitoring strategies for AC traction drives.

Thomas M. Wolbank (M' 1992) studied Industrial Electronics at the Vienna University of Technology in Austria where he also received the Doctor degree in 1996 and the Habilitation in 2004 respectively. At present he is with the Institute of Energy Systems and Electrical Drives at the Vienna University of Technology.
His research interests include saliency-based sensorless control of ac drives, dynamic properties and condition monitoring of inverter fed machines, transient electrical behaviour of ac machines, motor drives and their components, and controlling them by the use of intelligent control algorithms.
He has co-authored some 100 papers in refereed journals and international conferences.